J Appl Electrochem (2015) 45:273–280
DOI 10.1007/s10800-014-0786-8

RESEARCH ARTICLE

Electrochemical behavior of MgO-templated mesoporous carbons in the propylene carbonate solution of sodium hexafluorophosphate

Yuya Kado · Yasushi Soneda · Noriko Yoshizawa

Received: 28 August 2014 / Accepted: 29 December 2014 / Published online: 11 January 2015

Abstract MgO-templated mesoporous carbons annealed from 900 to 1,500 °C were examined as active materials for negative electrodes in a propylene carbonate electrolyte containing 1 M sodium hexafluorophosphate. The carbons annealed at 1,000 °C exhibited 180 mAh g^{-1} at a rate of 0.1 A g^{-1} in a potential range of 2.00–0.01 V versus Na^+/Na. The carbons showed good rate capability as well as cyclability. It is considered that mesopores plays a role of easy diffusion pathway for ions, and also significantly relates to both electric double layer capacitance and faradaic reactions involving Na ions. X-ray diffraction patterns, nuclear magnetic resonance spectra and Raman spectra were discussed for characterization of the carbons. Raman spectra indicated a reversible interaction of reduced Na with carbons. However, Na intercalation in the carbon layers was not confirmed for the carbon annealed at 1,000 °C. This is because the Na intercalation sites in the carbon layers are very few due to the disordered structure caused by the relatively low temperature annealing.

Keywords Mesoporous carbon · Rate performance · Organic electrolyte · Capacitive contribution

1 Introduction

Because of their excellent high power densities and long life cycles, electric double layer capacitors (EDLCs) have been widely used in power-assist systems of electric (hybrid) vehicles, cranes, memory back-up systems, and for load leveling of renewable energy [1–6]. However, the amount of energy that can be stored is limited by the energy storage mechanism of EDLCs, which involves non-faradaic adsorption/desorption of ions onto the electrode surface. The low energy density is an obstacle for using EDLCs as major power sources for large-energy applications such as electric vehicles. Introducing pseudocapacitance from faradaic reactions is one of the approaches used to increase the energy density of EDLCs [7–9]. A considerable number of studies have been done on pseudocapacitors using conducting polymers [10–12], metal oxides [13–15], and surface functional groups of carbon materials [16–18]. In addition, in recent years, lithium (Li) insertions for pseudocapacitance in electrode materials such as TiO_2 [19], MnO_3 [20], Fe_2O_3 [21, 22], and carbon [23, 24] have been explored because Li-based capacitors or batteries are very promising energy storage systems due to their high energy densities [25–28]. However, given the increasing demand for Li-based systems, there is concern about the depletion of Li resources, which are limited and unevenly distributed in the world. Thus, sodium (Na) has attracted interest as an alternative to Li for energy storage systems in view of its low cost and abundance (Na is 500 times more than Li in the Clarke number) [29–31]. In recent years, Na ion pseudocapacitors with metal oxide materials have been studied [32–34]. However, no type of carbon has been investigated for Na ion pseudocapacitor electrodes, although several researchers studied Na ion batteries with carbon materials such as hard carbons [35–42].

In the present study, electrochemical behaviors of MgO-templated mesoporous carbons (MPCs) with different crystallinities were examined in propylene carbonate solutions containing Na ions. MPCs are attractive electrode materials for EDLCs or batteries because of its unique

Y. Kado (✉) · Y. Soneda · N. Yoshizawa
Energy Technology Research Institute, National Institute of Advanced Industrial Science and Technology, 16-1 Onogawa, Tsukuba, Ibaraki 305-8569, Japan
e-mail: y.kado@aist.go.jp

properties, such as its mesopore-dominated structure with high specific surface areas and its simple production method [43–46]. They are produced by calcination of magnesium citrate and subsequent acid leaching of magnesia. The presence of mesopores enables high rate performances because of easy accessibility of the ions to the active surface of electrodes. Very recently, we have demonstrated that MPCs showed excellent rate performances for Na ion storage compared to commercial hard carbon materials [46]. In this work, we investigated the influence of crystallinity of MPCs, and discussed the advantage of mesoporous carbons in comparison to microporous activate carbons.

2 Experimental

The MgO-templated mesoporous carbon (CNovel®, annealed at 900 or 1,000 °C, Toyo Tanso Co., Ltd., denoted as MPC900, MPC1000) and carbons obtained by annealing of as-received MPC900 at 1,200 and 1,500 °C (expressed as MPC1200, MPC1500) were employed for the electrode materials. For comparison, we also used a commercially available activated carbon (YP-17, Kuraray Chemical Co., Ltd.). The carbon powders were mixed with styrene-butadiene rubber (SBR, BM-400B, Zeon, Co.) and carboxymethyl cellulose (CMC, D2200, Daicel FineChem Ltd.) at the ratio of 90:6:4 wt% in distilled water. The obtained slurry was doctor-bladed on an aluminum current collector. The thickness and loaded mass of the carbon layer were approximately 80 μm and 1 mg cm^{-2}. All the electrodes were fabricated with a diameter of 10 or 14 mm and used after dried overnight under vacuum at 120 °C. Carbon electrodes and glass fiber filters (GA-55, Toyo Roshi Kaisha, Ltd.) as separators were used after they were immersed in electrolytes for 30 min under reduced pressure. The electrolyte was 1 M sodium hexafluorophosphate (Wako Pure Chemical Industries, Ltd.) solution in propylene carbonate (Kanto Chemical Co., Ltd., electrochemistry grade). Electrochemical measurements were performed using a BioLogic VMP2 multi-channel galvanostat–potentiostat in a three electrode configuration. The carbons were used as the working electrodes, and Na metals were employed for the counter and reference electrode. The Na counter electrode was prepared with a diameter of 10 mm and a thickness of a few hundred micrometers. Charge/discharge tests were performed in a potential range of 2.00–0.01 V versus Na^+/Na at room temperature. Evaluation of the cyclability was performed in a two-electrode configuration with a coin type cell in the electrolyte containing 4 vol% of fluoroethylene carbonate (Tokyo Chemical Industry Co., Ltd.).

For characterization, the pore structures of the carbons were evaluated from adsorption/desorption isotherm of N_2 gas at 77 K using BELSORP-Max (BEL JAPAN, Inc.). Mesopore volumes, V_{meso}, and mesopore surface area, S_{meso}, were determined by BJH method. X-ray diffraction (XRD) patterns were recorded with a diffractometer (Bruker, D8 Advance) using Cu Kα radiation with a scanning range (2θ) from 15° to 35°. Raman spectra were acquired by in Via Raman microscope (Renishaw) with an Ar-ion laser (514.5 nm). In addition, MAS NMR measurements of ^{23}Na at room temperature were performed using a solid-state NMR spectrometer with a 7.0 T magnet (Chemagnetics, CMX-300) at 15 kHz spin rate in 4 mm diameter rotors. Chemical shifts were calibrated with respect to saturated NaCl aqueous solution, using a Na peak of solid NaCl at 7.21 ppm as an external reference. For NMR and Raman spectroscopy, carbon specimens were taken out from the cell at different charge levels and washed by propylene carbonate and acetonitrile in Ar atmosphere.

3 Results and discussion

3.1 N_2 isotherm

Figure 1a–e shows N_2 adsorption/desorption isotherms for the carbons. All the MPCs showed increase in adsorbed amount of N_2 at relatively high pressure regions, compared to commercial activated carbon (YP-17). This indicates the formation of mesopores for MPCs. BET surface areas and mesopore dimensions determined by the BJH method are summarized in Table 1. BET surface areas of MPCs are comparable to YP-17, but they decreased with elevation of annealing temperature. On the other hand, MPCs clearly have a large proportion mesopores. It should be noted that the MPCs possessed micropores as well as mesopores, as indicated by increase in N_2 adsorption at low pressures. In addition, the peak mesopore sizes for MPCs were around 3.8 nm, which was independent of annealing temperatures (Fig. 1f).

3.2 XRD and Raman spectroscopy for pristine carbon electrodes

Figure 2 shows (a) XRD and (b) Raman spectra for the pristine carbon electrodes. XRD patterns showed very broad peaks for all the carbons as shown in Fig. 2a, and no clear differences were observed for MPCs when they were annealed at 900–1,500 °C. This is ascribed to relatively low annealing temperature leading to disordered structures, and hence it is difficult to discuss the carbon structures with

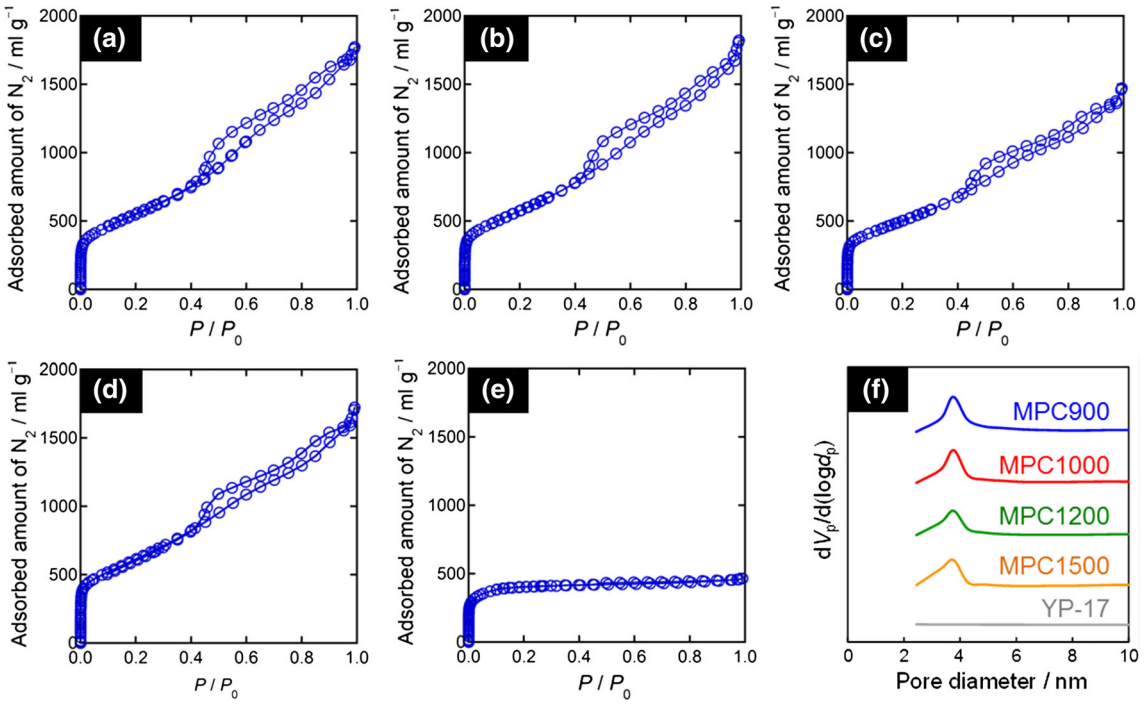

Fig. 1 N_2 adsorption/desorption isotherms at 77 K for **a** MPC900, **b** MPC1000, **c** MPC1200, **d** MPC1500, and **e** YP-17. **f** Mesopore size distributions for the carbons

Table 1 BET surface area, mesopore volume and mesopore surface areas of carbons

	S_{BET}/m^2 g^{-1}	V_{meso}/ml g^{-1}*	S_{meso}/m^2 g^{-1}*
MPC900	1,500	2.70	2,240
MPC1000	1,560	2.73	2,120
MPC1200	1,490	2.14	1,800
MPC1500	1,240	2.51	2,130
YP–17	1,500	0.15	140

* V_{meso} and S_{meso} were determined by BJH method

the XRD patterns. On the other hand, the Raman spectra showed a small difference for MPCs annealed at different temperatures (Fig. 2b). The broad peaks at around 1,350 and 1,580 cm^{-1} are the typical D and G bands, respectively. The peaks for YP-17 were as sharp as that for MPC900, and those for MPCs became sharper when annealed at higher temperatures. This indicates that the crystallinity of carbons was slightly enhanced by elevation of annealing temperature. The intensity for the D band increased with temperature increase, which is a known phenomenon in the carbonization temperature range [47].

3.3 Electrochemical measurements

Figure 3 shows cyclic voltammograms for the MPCs and YP-17. The reduction/oxidation peaks attributable to Na insertion/deinsertion were observed at around 0.1 V versus Na^+/Na for MPC1000, MPC1200 and MPC1500 (Fig. 3b–d). However, MPC900 and YP-17 showed unclear peaks, in particular, unclear oxidation peaks corresponding to Na deinsertion as shown in Fig. 3a, e. This result means that Na insertion/deinsertion is more reversible for the carbons annealed at higher temperatures. It is considered that higher-temperature annealing forms more local short-range ordered carbon layers and provides more Na intercalation sites in the carbon layers. Figure 4 shows the charge/discharge curves for these carbons. Small plateau potential regions were observed around 0.05 V versus Na^+/Na for MPC1200 and MPC1500. On the other hand, MPC900, MPC1000, and YP-17 showed no clear plateau potentials and relatively linear discharge (oxidation) curves, indicating capacitive behaviors. In addition, a shape difference between charge and discharge curves would be related to irreversibility, corresponding to the cyclic voltammograms. The irreversible capacity is most likely to originate from solid electrolyte interface (SEI) layer formation as discussed below [23, 24]. The discharge (oxidative) capacities of the carbons determined at the 5th cycle were plotted in Fig. 5. Figure 5a shows the discharge capacity in different potential ranges of 2.00–x (x = 0.01, 0.02, 0.05, 0.10, 0.20, 0.50, 0.75, 1.00, 1.25, and 1.50) V versus Na^+/Na, and Fig. 5b is the rate performances in the potential range of 2.00–0.01 V versus Na^+/Na. The discharge capacity was larger when the carbon was charged at more negative

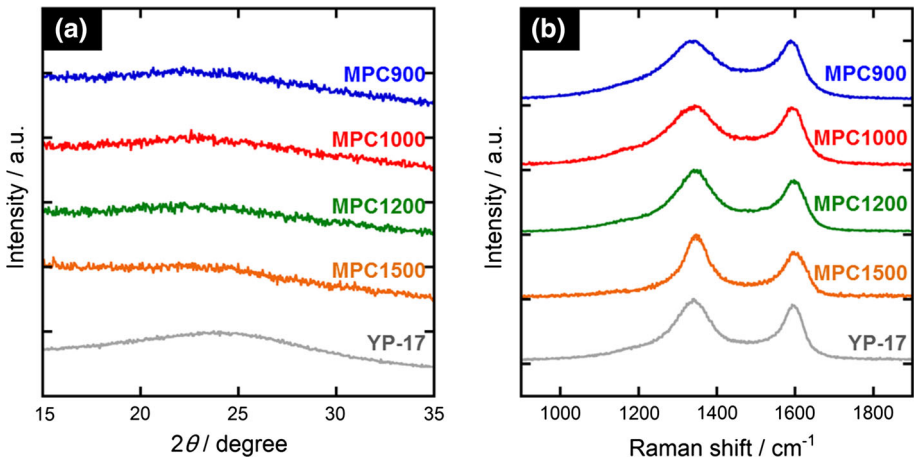

Fig. 2 **a** XRD and **b** Raman spectra for the MPC and YP-17 electrodes

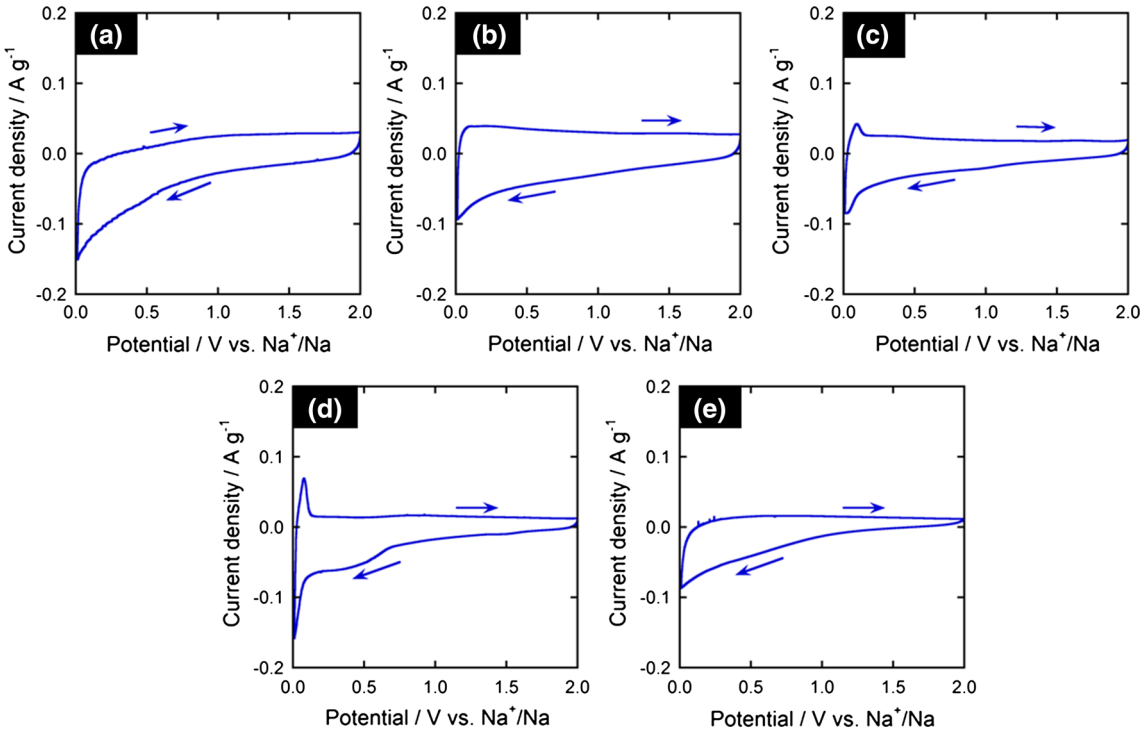

Fig. 3 Cyclic voltammograms in 1 M $NaPF_6$/PC electrolyte for **a** MPC900, **b** MPC1000, **c** MPC1200, **d** MPC1500, and **e** YP-17. The scan rate is 0.1 mV s^{-1}

potentials, and rapid increase in capacity was observed in more negative potentials than 0.1 V versus Na^+/Na. Among these carbons, MPC1000 showed the highest result reaching 180 mAh g^{-1} when it was charged to 0.01 V versus Na^+/Na. The CV curves suggested that faradaic Na insertion contributes to energy storage, but MPC1500 showed a smaller capacity than MPC1000 although the former has a higher crystallinity, in other words, a larger amount of intercalations sites for Na ion than the latter. This result indicates that capacitive contribution is also significant since MPC1000 has a larger specific surface area than MPC1500. In addition, MPCs exhibited much larger capacities than YP-17, indicating that mesopore plays an important role for Na ion storage. According to the previous work on Li insertion in porous carbons [23], Li cluster in the mesopores, rather than micropores, significantly contribute to the Li ion storage. It is hence analogically deduced that the charge storage arises from the charge transfer between carbons and Na clusters formed in the mesopores. Another conceivable reason for the low capacity of YP-17 is pore filling by SEI layer formation since activated carbon mainly comprises

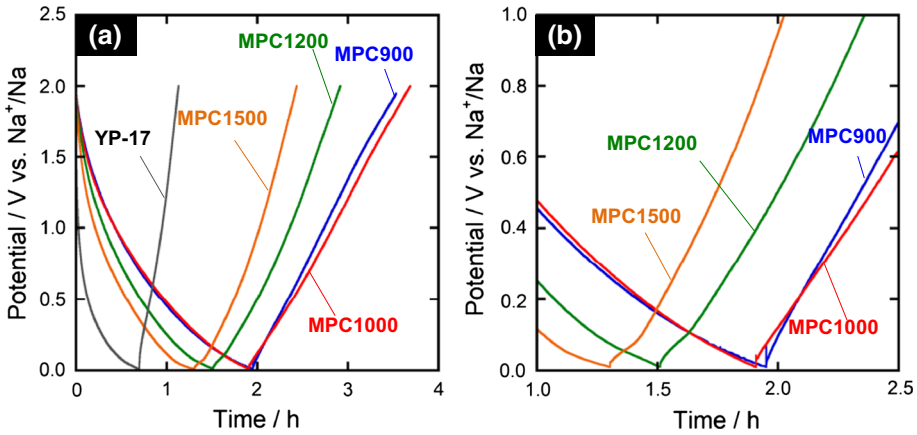

Fig. 4 Charge/discharge curves (5th cycle) at 0.1 A g^{-1} in a potential range of 2.00–0.01 V versus Na^+/Na in 1 M $NaPF_6$/PC electrolyte. **b** is a magnification of negative potential regions of (**a**)

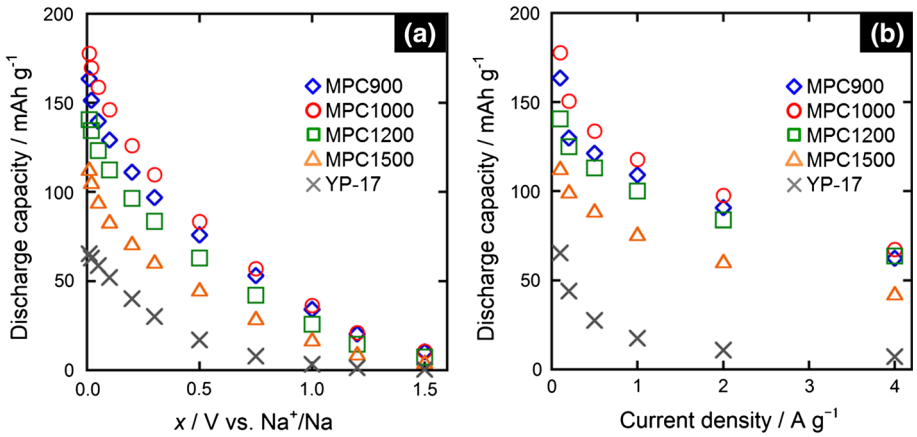

Fig. 5 Discharge (oxidative) capacity acquired at 0.1 A g^{-1} in various potential ranges of 2.00–x (x = 0.01, 0.02, 0.05, 0.10, 0.20, 0.50, 0.75, 1.00, 1.25, and 1.50) V versus Na^+/Na. **b** Rate performances in the range of 2.00–0.01 V versus Na^+/Na in 1 M $NaPF_6$/PC electrolyte

micropores. Furthermore, MPCs showed a remarkable rate capability, and MPC1000 reached 70 mAh g^{-1} at 4 A g^{-1} as shown in Fig. 5b. This is ascribed to easy accessibility of the ions to the active surface in the mesopores. The capacity of YP-17 decreased with an increase in current density, and is quite low at high rates because of the low conductivity of the electrode and the high diffusion resistance of the ions in the micropores. Cyclability of MPC1000, which showed the largest capacity, was evaluated in the electrolyte containing 4 vol% of FEC. It is known that FEC addition to the PC-based electrolyte is effective for formation of stable SEI layers [37]. Figure 6 shows the capacity retention (a ratio of the capacity at each cycle to that at the first cycle), and coulombic efficiency. The capacity retention decreased in the beginning of cycles. However, the retention showed an almost constant value after 100 cycles, and 89 % remained after 1,000 cycles. Moreover, the coulombic efficiency reached 99.9 % after 100 cycles, although the first cycle showed a very low efficiency. The low efficiency of the first cycle reflects the large irreversible capacity, which is considered to originate from SEI layer formation. Because MPCs has a large amount of mesopores, solvated Na cations can easily move

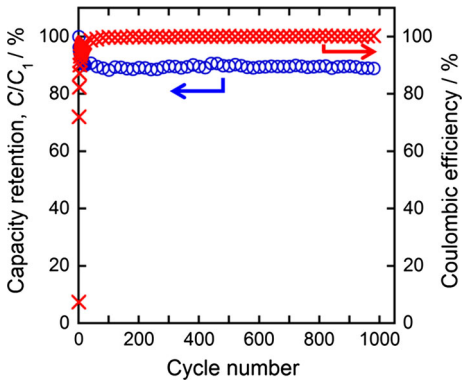

Fig. 6 Capacity retention and coulombic efficiency for MPC1000 acquired at 0.1 A g^{-1} in the potential range of 2.00–0.01 V versus Na^+/Na in 1 M $NaPF_6$/(PC-4 vol% FEC) electrolyte

to the active surfaces of carbons where they are decomposed to form the SEI layers [23, 39]. Thus, mesopores represented a significant Na ion storage, but, at the same time, a drawback of a large irreversible capacity. Reduction of the irreversible capacity is an important requirement for practical application, and further investigations are in progress.

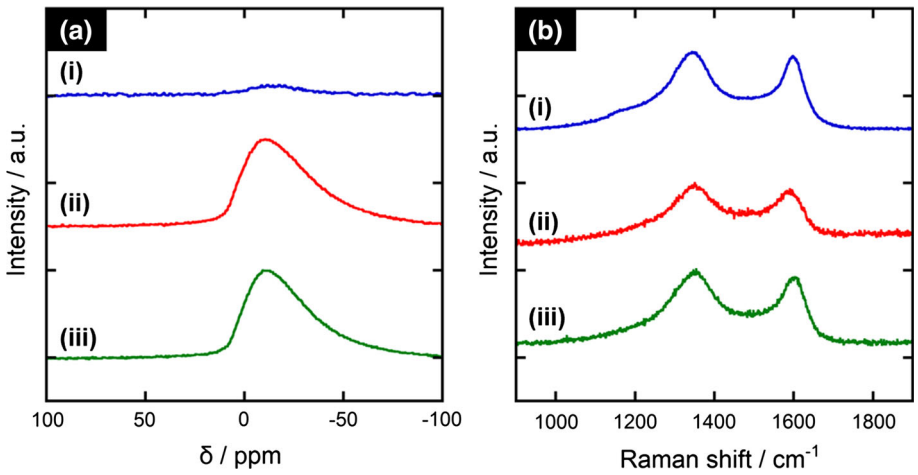

Fig. 7 **a** ^{23}Na NMR and **b** Raman spectra for MPC1000 at different charge levels: electrochemically reduced to (*i*) 2.00 V, (*ii*) 0.01 V, and (*iii*) oxidized to 2.00 V after the first reduction to 0.01 V versus Na^+/Na

3.4 NMR and Raman spectroscopy for the charged/discharged carbons

NMR and Raman spectroscopy were conducted to examine Na insertion in the MPC1000 electrode. Figure 7a shows the ^{23}Na MAS NMR spectra for MPC1000, which was electrochemically reduced to 2.0, 0.01 V, and oxidized to 2.0 V after the first reduction to 0.01 V versus Na^+/Na. No peak was observed for the carbon obtained at 2.0 V versus Na^+/Na; however, a very broad peak appeared between +10 and −50 ppm for MPC1000 reduced to 0.01 V versus Na^+/Na. According to the literature [36, 42], a signal at +9 ppm is ascribed to Na inserted between misaligned carbon layers, and a broad peak at −20 to −30 ppm is due to Na inserted in nanocavities and in SEI layers. The obtained broad peak comprises all these signals and others whose origins are unknown. Na cluster in the mesopores could also contribute to the broad signal [23]. However, a broad peak remained for the carbon obtained at 2.0 V after the first reduction to 0.01 V versus Na^+/Na as shown in Fig. 7a(iii). This means that Na insertion/deinsertion in MPC1000 includes an irreversible process, i.e., the broad peak mainly arises from the SEI layer formation and the signals from other components are very small. On the other hand, as shown in Fig. 7b, the Raman spectrum for MPC1000 reduced to 0.01 V versus Na^+/Na was slightly broadened in comparison to that for the carbon obtained at 2.0 V. In addition, the carbon oxidized to 2.0 V after the first reduction to 0.01 V showed as a sharp peak as the carbon obtained at 2.0 V without reduction. This result indicates that reduced Na has some interactions with the carbons, and the interaction process is reversible. Moreover, no peak shift was observed in the spectra for the carbon reduced to 0.01 V, and Na intercalation in the carbon layers was not confirmed. It is considered that the Na intercalation sites in the carbon layers are very few because of the disordered structure caused by the relatively low temperature annealing (1,000 °C). Thus, the main reaction in the beginning of the cycles was the SEI layer formation, but a partially reversible phenomenon was confirmed by Raman spectroscopy. No clear evidence of reversible Na insertion in the carbons was observed.

4 Conclusions

This paper presents electrochemical behaviors of MgO-templated mesoporous carbons in a propylene carbonate electrolyte containing Na ions. The mesoporous carbons annealed at 1,000 °C exhibited the highest capacity, good rate capability as well as good cyclability. It is considered that existence of mesopores in the carbon is an origin of the large irreversible capacity, but also significantly contributes to Na ion energy storage: combination of electric double layer capacitance and reduction/oxidation involving Na ions. Although further investigations on reducing irreversible capacity are required to enable practical application, we believe that easy accessibility of the ions to the electrode surface and the significant capacitive contribution of mesoporous materials with high specific surface areas are promising properties for further improvement in the energy storage systems.

Acknowledgments We would like to thank Dr. T. Morishita, Toyo Tanso CO., Ltd., for supplying the MgO-templated mesoporous carbons and also greatly appreciate Dr. H. Kawashima at AIST for performing the ^{23}Na NMR measurements.

References

1. Conway BE (1999) Electrochemical supercapacitors: scientific fundamentals and technological applications. Kluwer Academic/Plenum Publisher, New York
2. Simon P, Gogotsi Y (2008) Materials for electrochemical capacitors. Nat Mater 7:845–854

3. Frackwiak E, Béguin F (2001) Carbon materials for the electrochemical storage of energy in capacitors. Carbon 39:937–950
4. Miller JR, Simon P (2008) Science 321:651–652
5. Kötz R, Carlen M (2000) Principles and applications of electrochemical capacitors. Electrochim Acta 45:2483–2498
6. Inagaki M, Konno H, Tanaike O (2010) J Power Sour 195:7880–7903
7. Naoi K, Simon P (2008) New materials and new configurations for advanced electrochemical capacitors. J Electrochem Soc 17:34–37
8. Conway BE (1991) Transition from "supercapacitor" to "battery" behavior ion electrochemical energy strorage. J Electrochem Soc 138:1539–1548
9. Conway BE, Birss V, Wojtowicz J (1997) The role and utilization of pseudocapacitance for energy storage by supercapacitors. J Power Sour 66:1–14
10. Ryu KS, Kim KM, Park NG, Park YJ, Chang SH (2002) Symmetric redox supercapacitor with conducting polyaniline electrodes. J Power Sour 103:305–309
11. Rudge A, Davey J, Raistrick I, Gottesfeld S, Ferrais JP (1994) Conducting polymers as active materials in electrochemical capacitors. J Power Sour 47:89–107
12. Laforgue A, Simon P, Sarrazin C, Fauvarque JF (1999) Polythiophene-based supercapacitors. J Power Sour 80:142–148
13. Toupin M, Brousse T, Bélanger D (2004) Charge storage mechanism of MnO_2 electrode used in aqueous electrochemical capacitor. Chem Mater 16:3184–3190
14. Liu KC, Anderson MA (1996) Porous nickel oxide/nickel films for electrochemical capacitors. J Electrochem Soc 143:124–130
15. Zheng JP, Cygan PJ, Jow TR (1995) Hydrous ruthenium oxide as an electrode material for electrochemical capacitors. J Electrochem Soc 142:2699–2703
16. Frackowiak E, Lota G, Machnikowski J, Guterl CV, Béguin F (2006) Optimisation of supercapacitors using carbons with controlled nanotexture and nitrogen content. Electrochim Acta 51:2209–2214
17. Raymundo EP, Leroux F, Béguin F (2006) A high-Performance carbon for supercapacitors obtained by carbonization of a seaweed biopolymer. Adv Mater 18:1877–1882
18. Kodama M, Yamashita J, Soneda Y, Hatori H, Kamegawa K (2007) Preparation and electrochemical characteristics of N-enriched carbon foam. Carbon 45:1105–1107
19. Wang J, Polleux J, Lim J, Dunn B (2007) Pseudocapacitive contributions to electrochemical energy storage in TiO_2 (anatase) nanoparticles. J Phys Chem C 111:14925–14931
20. Brezesinski T, Wang J, Tolbert SH, Dunn B (2010) Ordered mesoporous α-MoO_3 with iso-oriented nanocrystalline walls for thin-film pseudocapacitors. Nat Mater 9:146–151
21. Brezesinski K, Haetge J, Wang J, Mascotto S, Reitz C, Rein S, Tolbert SH, Perlich J, Dunn B, Brezesinski T (2011) Ordered mesoporous α-Fe_2O_3 (hematite) thin-film electrodes for application in high rate rechargeable lithium batteries. Small 7:407–414
22. Karthikeyan K, Amaresh S, Lee SN, Aravindan V, Lee YS (2014) Fluorine-doped Fe_2O_3 as high energy density electroactive material for hybrid supercapacitor applications. Asian J 9:852–857
23. Frackwiak E, Béguin F (2002) Electrochemical storage of energy in carbon nanotubes and nanostructured carbons. Carbon 40:1775–1787
24. Frackowiak E, Gautier S, Gaucher H, Bonnamy S, Béguin F (1999) Electrochemical storage of lithium multiwalled carbon nanotubes. Carbon 37:61–69
25. Nishi Y (2001) J Power Sour 100:101–106
26. Tarascon JM, Armand M (2001) Issues and challenges facing rechargeable lithium batteries. Nature 414:359–367
27. Armand M, Tarascon JM (2008) Building better batteries. Nature 451:652–657
28. Palacin MR (2009) Recent advances in rechargeable battery materials: a chemist's perspective. Chem Soc Rev 38:2565–2575
29. Kim SW, Seo DH, Ma X, Ceder G, Kang K (2012) Electrode materials for rechargeable sodium-ion batteries potential alternatives to current lithium-ion batteries. Adv Energy Mater 2:710–721
30. Slater MD, Kim D, Lee E, Johnson CS (2013) Sodium-ion batteries. Adv Funct Mater 23:947–958
31. Clarke FW, Washingtonarth HS (1922) The average chemical composition of igneous rocks. Proc Natl Acad Sci USA 8(5):108–115
32. Chen Z, Augustyn V, Jia X, Xiao Q, Dunn B, Lu Y (2012) High-performance sodium-ion pseudocapacitors based on hierarchically porous nanowire composites. ACS Nano 6:4319–4327
33. Patel MN, Wang X, Wilson B, Ferrer DA, Dai S, Stevenson KJ, Johnston KP (2010) Hybrid MnO_2–disordered mesoporous carbon nanocomposites: synthesis and characterization as electrochemical pseudocapacitor electrodes. J Mater Chem 20:390–398
34. Liang R, Cao F, Qian D (2011) MoO_3 nanowires as electrochemical pseudocapacitor materials. Chem Commun 47:10305–10307
35. Stevens DA, Dahn JR (2000) High capacity anode materials for rechargeable sodium-ion batteries. J Electrochem Soc 147:1271–1273
36. Alcántara R, Lavela P, Ortiz JF, Tirado JL (2005) Carbon microspheres obtained from resorcinol-formaldehyde as high-capacity electrodes for sodium-ion batteries. Electrochem Solid-State Lett 8:A222–A225
37. Komaba S, Ishikawa T, Yabuuchi N, Murata W, Ito A, Ohsawa Y (2011) Fluorinated ethylene carbonate as electrolyte additive for rechargeable Na batteries. ACS Appl Mater Interfaces 3:4165–4168
38. Komaba S, Murata W, Ishikawa T, Yabuuchi N, Ozeki T, Nakayama T, Ogata A, Gotoh K, Fujiwara K (2011) Electrochemical Na insertion and solid electrolyte interphase for hard-carbon electrodes and application to Na-ion batteries. Adv Funct Mater 21:3859–3867
39. Wenzel A, Hara T, Janek J, Adelhelm P (2011) Room-temperature sodium-ion batteries Improving the rate capability of carbon anode materials by templating strategies. Energy Environ Sci 4:3342–3345
40. Cao Y, Xiao L, Sushko ML, Wang W, Schwenzer B, Xiao J, Nie Z, Saraf LV, Yang Z, Liu J (2012) Sodium ion insertion in hollow carbon nanowires for battery applications. Nano Lett 12:3783–3787
41. Tang K, Fu L, White RJ, Yu L, Titirici M, Antonietti M, Maier J (2012) Hollow carbon nanospheres with superior rate capability for sodium-based batteries. Adv Energy Mater 2:873–877
42. Gotoh K, Ishikawa T, Shimazu S, Yabuuchi N, Komaba S, Takeda K, Goto A, Deguchi K, Ohki S, Hashi K, Shimizu T, Ishida H (2013) NMR study for electrochemically inserted Na in hard carbon electrode of sodium ion battery. J Power Sour 225:137–140
43. Morishita T, Tsumura T, Toyoda M, Przepiórski J, Morawski AW, Konno H, Inagaki M (2010) A review of the control of pore structure in MgO-templated anoporous carbons. Carbon 48:2690–2707

44. Morishita T, Soneda Y, Tsumura T, Inagaki M (2006) Preparation of porous carbons from thermoplastic precursors and their performance for electric double layer capacitors. Carbon 44:2360–2367
45. Soneda Y, Kodama M (2013) Effect of mesopore in MgO templated mesoporous carbon electrode on capacitor performance. Electrochemistry 81:845–848
46. Kado Y, Soneda Y, Yoshizawa N (2015) Excellent rate capability of MgO-templated mesoporous carbon as an Na-ion energy storage material. ECS Electrochem Lett 4:A22–A23
47. Rouzaud JN, Deldicque D (2014) Structural study of carbonization process: a field for Raman microspectrometry. Carbon 2014 Conference Extended Abstract: ORT7-13, Jeju, Korea, June 29–July 4